Current Science
CS 6 (2), 6006-6018 (2026)
Received 30 January 2026 | **Accepted 12 March** 2026 | **Online Available 16 March** 2026
https://doi.org/10.52845/CS/2026-6-2-3

Current Science

Current Science

OPEN ACCESS

ISSN (O) 2795-8639

Original Article

A Numerical Study of the Impact of Solar Radiation on the Temperature and Airflow Fields in Hospital Wards

Wang Leilei[1], Xia Jiangling[2]*

[1]School of Building Engineering, Zibo Polytechnic University, Zibo, Shandong, P.R. China

[2]Department of Anesthesiology, Zibo Central Hospital, Zibo,Shandong, P.R. China

***Corresponding Author: Xia Jiangling**

Abstract:
Post the COVID-19 pandemic, healthcare has become a key public concern, and medical environment quality requirements have grown stricter. New hospital wards often adopt a large window-to-wall ratio for natural lighting, but this may cause uneven temperature and draft discomfort in hot-summer and cold-winter regions' air-conditioned wards. This study takes a standard double-bed ward as the object, establishing a physical model via GAMBIT and conducting FLUENT simulations with the S2S radiation model and Realizable k-ε model. It analyzes temperature and airflow fields under Summer/Winter Solstice solar radiation and compares them with non-radiation conditions. Results show the human core activity zone (0.7m-1.9m) is weakly affected by solar radiation: summer cooling brings 293.0K-293.8K and 0.04-0.12m/s, winter heating 288.0K-289.0K and 0.02-0.06m/s, all meeting GB/T 50736-2012. However, the upper zone (>2m) suffers significant airflow acceleration and temperature fluctuations due to thermal buoyancy, reducing air conditioning efficiency. This study provides scientific references for ward air conditioning optimization and bed layout.

Keywords: Hospital ward; Solar radiation; Temperature and airflow field; Numerical simulation; Thermal comfort; Hot-summer and cold-winter region

Introduction

In the post-pandemic era, healthcare has emerged as a core public concern, and the thermal comfort and safety of medical environments have attracted growing attention [1-4]. To optimize the lighting conditions in wards, the exterior walls of newly built hospital wards generally adopt a large window-to-wall ratio design to enhance the intensity and duration of solar radiation. However, in hot-summer and cold-winter regions, this design may interact with the heating/cooling functions of central air conditioning systems, leading to disordered indoor airflow organization, uneven temperature distribution, and subsequent draft discomfort for occupants [5-8].

Numerous studies have been conducted on the airflow organization in hospital wards. Zhiqiang Kang et al. [9] used CFD software to investigate the impact of air supply outlet positions on the temperature and velocity fields in wards. Jin Xuening [10] employed Fluent for simulation calculations and concluded that changes in the positions of air supply and exhaust outlets, as well as the sizes of air supply and return outlets, affect indoor pollutant distribution. Ru Zihao [11] analyzed the indoor thermal comfort parameters of personalized air conditioning schemes using FLUENT software. Chen Hongfeiran [12] took container-modified isolation wards as the research object and studied the influence of air supply angles on the thermal and pollutant environments under different outdoor temperatures. Wang Leilei et al. [13] simulated the effect of air outlet

positions on the distribution of temperature and velocity fields in standard double-bed wards of a newly built hospital. Despite the valuable insights gained from these studies, none have considered the combined effect of solar radiation and air conditioning systems on the temperature and velocity fields in wards in hot-summer and cold-winter regions, nor have they proposed targeted recommendations for bed installation based on such considerations.

Therefore, this study focuses on a standard double-bed general ward of a newly built hospital in a hot-summer and cold-winter region. Considering the influence of solar radiation on the Summer Solstice and Winter Solstice, numerical simulations were performed using FLUENT software to systematically analyze the distribution patterns of the temperature and velocity fields in the ward. The aim is to provide theoretical support for the optimization of ward air conditioning design and the rational layout of hospital beds.

2 Ward Model and Numerical Methods

2.1 Physical Model

A standard double-bed general ward of a newly built hospital was selected as the research prototype, with the following geometric parameters: depth of 9.0m, width of 4.0m, floor height of 3.9m, ceiling height at the entrance of 2.9m, and a glass curtain wall on the south side. During modeling, the influences of glass curtain wall mullions, entrance doors, and hospital beds (with dimensions of 2000mm×1000mm×700mm), which have minimal impact on airflow organization, were ignored to simplify the calculation. The ward adopts a side supply and upper return air distribution mode, with the fan coil unit and fresh air system concealed in the ceiling at the entrance. The heights of the air supply outlet and fresh air outlet are 3.0m, and the height of the return air outlet is 2.9m. The dimensions of the air supply outlet, fresh air outlet, and return air outlet are 150mm×850mm, 200mm×200mm, and 400mm×200mm, respectively. To improve model accuracy and facilitate mesh generation, GAMBIT software was used to establish the physical model, with the positive X-direction defined as east, the positive Y-direction as north, and the positive Z-direction as the vertical height of the ward.

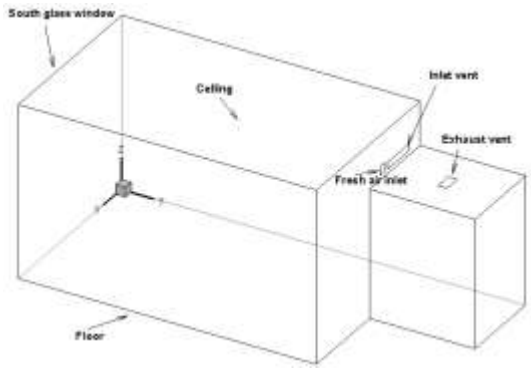

Figure 1. Physical Model

2.2 Mathematical Model

To simplify the problem, the following assumptions were made: (1) The air in the ward is incompressible and satisfies the Boussinesq hypothesis; (2) The flow is steady-state turbulence; (3) Air leakage through door and window gaps is negligible; (4) Indoor air is a radiation-transparent medium. The geographical

location and time zone of the research object were set, and solar radiation simulation on the Summer Solstice was conducted using a solar ray tracing model under clear sky conditions. Based on the characteristics of fluid motion in the physical model, the Surface-to-Surface (S2S) radiation model and the Realizable k-ε three-dimensional turbulent model were adopted for numerical simulation [8].

$$\rho \frac{dk}{dt} = \frac{\partial}{\partial x_i}\left[\left(\mu + \frac{\mu_i}{\sigma_k}\right)\frac{\partial k}{\partial x_i}\right] + G_k + G_b - \rho\varepsilon - Y_M \quad (1)$$

$$\rho \frac{\mathrm{d}\varepsilon}{\mathrm{d}t} = \frac{\partial}{\partial x_i}\left[\left(\mu + \frac{\mu_t}{\sigma_\varepsilon}\right)\frac{\partial \varepsilon}{\partial x_i}\right] + \rho C_1 S\varepsilon - \rho C_2 \frac{\varepsilon^2}{k+\sqrt{\nu\varepsilon}} + C_{1\varepsilon}\frac{\varepsilon}{k}C_{3\varepsilon}G_b \quad (2)$$

In the equations, $C_1 = max\left[0.43, \frac{\eta}{\eta+5}\right]$, $\eta = Sk/\varepsilon$

Among them, G_k denotes the turbulent kinetic energy production caused by the mean velocity gradient; G_b denotes the turbulent kinetic energy production induced by the buoyancy effect; Y_M represents the influence of compressible turbulent pulsation expansion on the total dissipation rate; $C_{2\varepsilon}$ and $C_{1\varepsilon}$ are constants; σ_k and σ_ε are the turbulent Prandtl numbers for turbulent kinetic energy and its dissipation rate, respectively. In the calculation, $C_{1\varepsilon}$ =1.44 , $C_{2\varepsilon}$ =1.9 , σ_k =1.0 , and σ_ε =1.2 .

In the S2S radiation model, the radiation leaving a surface consists of its own emission and the reflection of incident radiation. The reflected part depends on the incident radiation from surrounding objects, which can be expressed as the sum of the radiative heat fluxes emitted by other surfaces. For surface k, the total radiative heat flux emitted is given by:

$$q_{out,k} = \varepsilon_k \sigma T_k^4 + \rho_k q_{in,k} \quad (3)$$

Among them, $q_{out,k}$ denotes the total radiative heat flux leaving surface k , ε_k is the emissivity, σ is the Stefan-Boltzmann constant, ρ_k is the reflectivity, and $q_{in,k}$ is the incident radiative heat flux emitted by surrounding objects. Define the view factor F_{jk}, as the fraction of the radiation leaving surface k that is received by surface j . Then, the incident radiative heat flux on surface k can be expressed as a function of the radiative heat fluxes leaving the other surfaces:

$$A_k q_{in,k} = \sum_{j=1}^{N} A_j q_{out,j} F_{jk} \quad (4)$$

where A_k is the area of surface k , and F_{jk} is the view factor from surface j to surface k . For n surfaces, the reciprocity relation of view factors gives:

$$A_j F_{jk} = A_k F_{kj}, j = 1,2,3,...N \quad (5)$$

$$\text{Thus: } q_{in,k} = \sum_{j=1}^{N} F_{kj} q_{out,j} \quad (6)$$

$$\text{And: } q_{out,k} = \varepsilon_k \sigma T_k^4 + \rho_k \sum_{j=1}^{N} F_{kj} q_{out,j} \quad (7)$$

$$\text{Equation (7) above can be simplified as: } J_k = E_k + \rho_k \sum_{j=1}^{N} F_{kj} J_j \quad (8)$$

where J_k represents the radiosity emitted from surface k , and E_k represents the intrinsic radiation of surface k .

2.3 Simulation Assumptions and Boundary Conditions

Solar radiation enters the ward through the south-facing external window and is absorbed and reflected by the window, walls, and floor. The external window conducts radiative and convective heat transfer with the indoor and outdoor environments, thus being set as a mixed thermal boundary. The outdoor ambient temperature was taken as the statistical average of Zibo area on June 21st (13:00) of the Summer Solstice and December 21st (07:00) of the Winter Solstice over the years, while the indoor temperature was set to the design temperatures for summer cooling and winter heating in the ward. The internal walls, floor, and ceiling do not directly exchange heat with the external environment and are assumed to be isothermal boundaries consistent with the indoor design temperatures. Due to the small temperature difference between indoor and outdoor, the convective heat transfer coefficients between the external window and indoor/outdoor air were set to the same constant value. The air supply outlet and fresh air outlet of the fan coil unit were defined as velocity inlets, and the return air outlet as a free outflow. The heat sources from indoor lighting and personnel were ignored. The specific boundary condition parameters for summer cooling and winter heating are presented in Tables 1 and 2.

Table 1 Boundary condition parameters of the calculation model during summer cooling

No.	Name of Boundary Condition	Type of Boundary Condition	Boundary Condition Value
1	Internal walls, floor, and ceiling	Isothermal boundary	299K Internal emissivity = 0.8
2	External window	Mixed thermal boundary	Heat transfer coefficient = 4 W/(m²·K) Internal air temperature = 299K External emissivity = 0.49 External radiant temperature = 308.5K Internal emissivity = 0.8
3	Air supply outlet of fan coil unit	Velocity inlet	1.05m/s, 286.5K
4	Fresh air inlet	Velocity inlet	0.56m/s, 308.5K
5	Return air outlet	Free outflow	——
6	Geographical location and time	——	Longitude = 118°

	zone		Latitude = 36° Timezone = GMT+8
7	Calculation time of solar radiation	——	13:00 on June 21st

Table 2 Boundary condition parameters of the calculation model during winter heating

No.	Name of Boundary Condition	Type of Boundary Condition	Boundary Condition Value
1	Internal walls, floor, and ceiling	Isothermal boundary	297K Internal emissivity = 0.8
2	External window	Mixed thermal boundary	Heat transfer coefficient = 4 W/(m²·K) Internal air temperature = 299K External emissivity = 0.49 External radiant temperature = 267K Internal emissivity = 0.8
3	Air supply outlet of fan coil unit	Velocity inlet	1.05m/s, 299K
4	Fresh air inlet	Velocity inlet	0.56m/s, 267K
5	Return air outlet	Free outflow	——
6	Geographical location and time zone	——	Longitude = 118° Latitude = 36° Timezone = GMT+8
7	Calculation time of solar radiation	——	07:00 on December 21st

2.4 Numerical Calculation Method

Firstly, the physical model was meshed using Gambit, with grid refinement performed around the air outlets and their adjacent areas, resulting in a total of 820,817 computational grids (as shown in Figure 2). Subsequently, numerical simulations were carried out using FLUENT software. The SIMPLEC algorithm was employed for the coupling of velocity and pressure fields to solve the steady-state problem of incompressible fluid. Different horizontal planes along the vertical Z-direction (0.7m, 0.9m, 1.1m, 1.3m, 1.5m, 1.7m, 1.9m) were selected to investigate the distribution of temperature and velocity fields in the ward under the given boundary conditions, with a focus on the human activity zone and the area around the bed height.

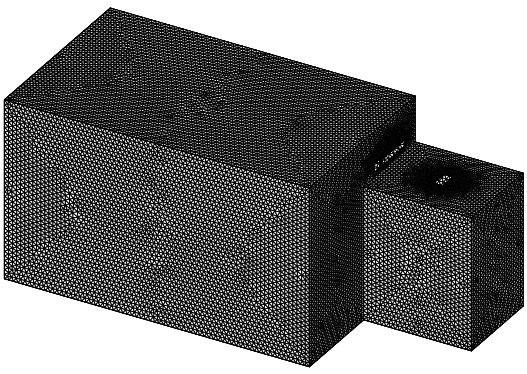

Figure 2. Computational Grids

3 Results and Analysis

3.1 Distribution Characteristics of Temperature Field

3.1.1 Summer Cooling Condition

Under summer cooling conditions, the indoor temperature exhibits a vertical distribution pattern of "stable at low levels, transitional at medium levels, and increasing at high levels" (Figure 3). The temperature in the human core activity zone (0.7m-1.9m) ranges from 293.0K to 293.8K with a fluctuation amplitude of ≤0.8K, meeting the thermal comfort requirements specified in GB/T 50736-2012[14]. The temperature gradient from the near-ground area to the lower part of the core zone (0.7m-1.3m) is ≤0.3K/m, indicating that the cold air sinking effect is notvious and the air supply diffuses uniformly in this region. The height range of ob1.5m-1.7m serves as a transitional zone, where the temperature gradient increases from 0.3K/m to 0.5K/m, acting as the mixing interface between cold and rising hot air. Although the temperature fluctuation in this zone is slightly larger than that in the core activity zone, it does not affect the overall comfort. For the upper zone above 2.0m, the temperature rises rapidly, reaching above 294.5K at 3.0m, with a temperature difference of ≥0.7K compared to 1.9m, showing a significant hot air accumulation phenomenon, which is a typical characteristic of natural upward movement of indoor heat driven by thermal buoyancy.

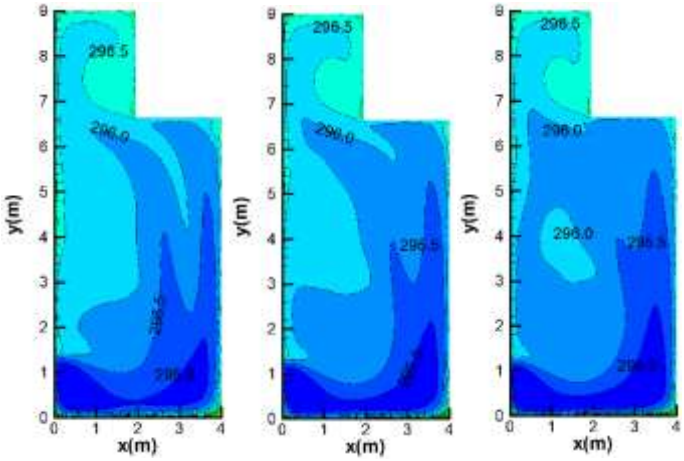

a) Z=0.7m **b) Z=0.9m** **c) Z=1.1m**

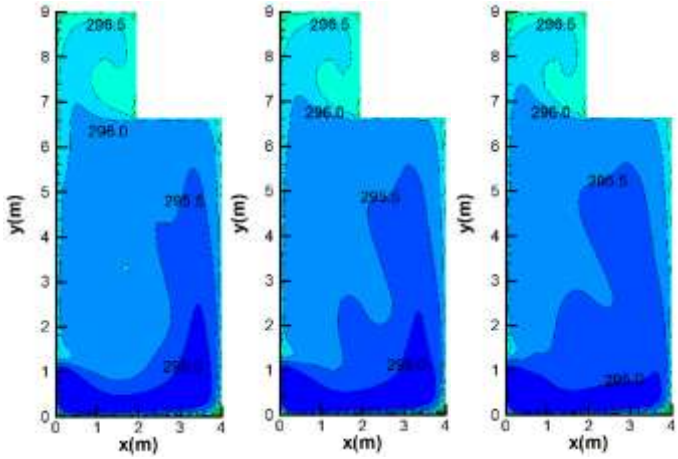

d) Z=1.3m **e) Z=1.5m** **f) Z=1.7m**

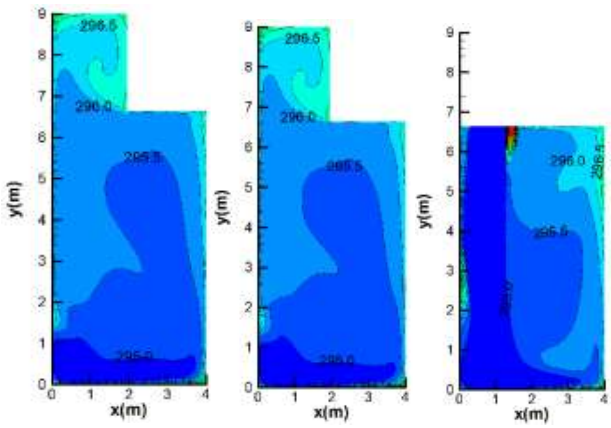

g) Z=1.9m h) Z=2.0m j) Z=3.0m

Figure 3 Temperature field distributions at different Z-values under summer cooling conditions (Unit: K)

In the horizontal direction, most areas of the core activity zone exhibit good temperature uniformity with a horizontal temperature difference of ≤0.5K. Slight temperature heterogeneity (temperature difference of 0.6K-0.8K) occurs in local areas such as near external walls, furniture, and air outlets, which is presumably caused by obstructed airflow or incomplete diffusion of supply air jets, but no obvious high or low-temperature dead zones are formed. In the upper zone, the horizontal temperature difference increases significantly (maximum temperature difference ≥1.2K), and high-temperature accumulation zones are formed in room corners and under the ceiling, mainly due to the low air velocity and insufficient heat exchange in this region.

3.1.2 Winter Heating Condition

Under winter heating conditions, the indoor temperature presents a vertical stratification characteristic of "cold at low levels and hot at high levels" (Figure 4). The temperature in the human core activity zone (0.7m-1.9m) ranges from 288.0K to 289.0K, but the near-ground area (0.7m-1.1m) has a lower temperature (287.5K-288.0K), with a temperature difference of 1.0K-1.5K compared to the upper zone (2.0m-3.0m). This reflects the "thermal stratification" phenomenon caused by hot air rising, indicating that the heating air flow has insufficient sinking capacity and fails to fully cover the near-ground area. The temperature in the upper zone (2.0m-3.0m) increases significantly to 289.0K-289.5K, showing obvious hot air accumulation.

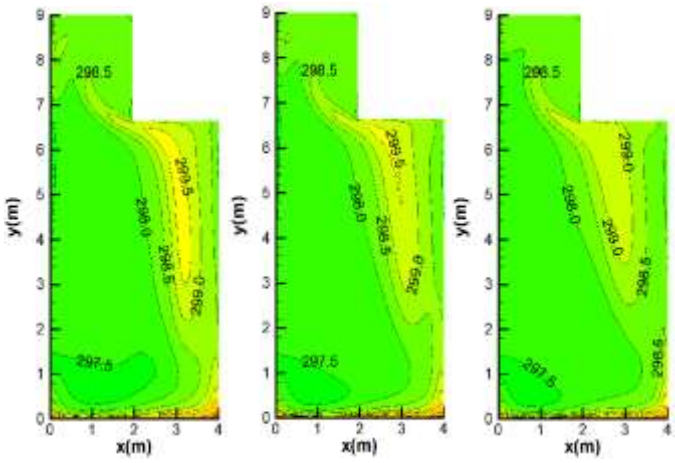

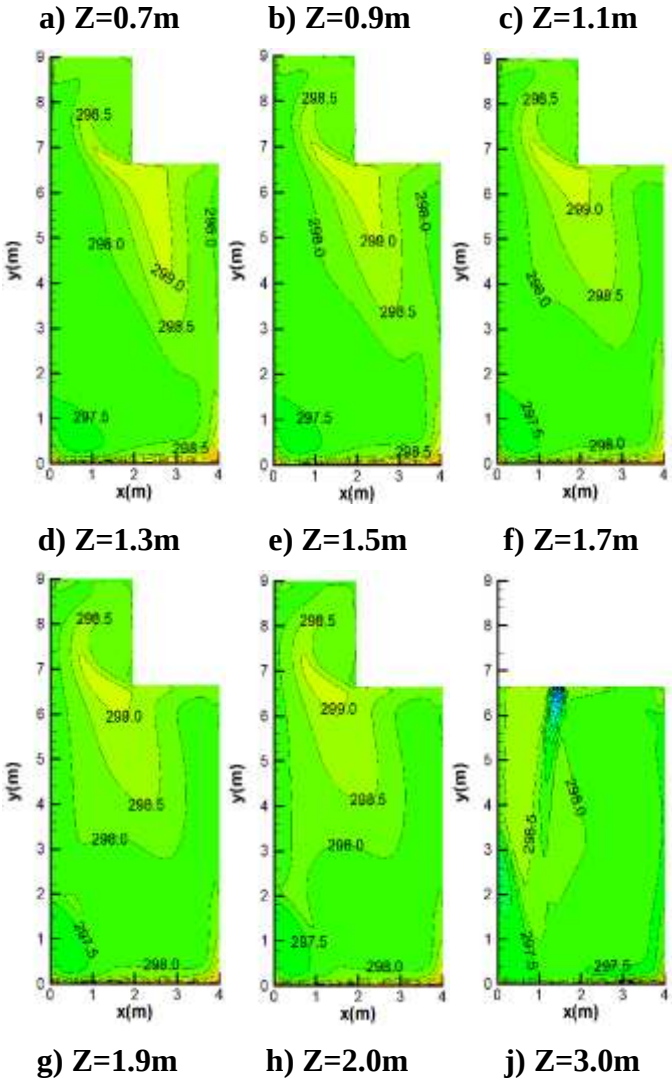

Figure 4 Temperature field distributions at different Z-values under winter heating conditions (Unit: K)

In the horizontal direction, the left area of the core activity zone (x≈1, y≈3-7) has a large temperature gradient (287.5K-289.0K), exhibiting "uneven temperature distribution". The right area (x≈3-4) has relatively uniform temperature (288.5K-289.0K), but due to being an uncovered area of the heating air supply, there is heat loss through the wall, leading to uneven horizontal temperature distribution. The horizontal temperature difference in the upper zone further expands (288.5K-289.5K), with high-temperature zones concentrated in the upper corners of the room, where slow airflow exacerbates temperature unevenness.

3.2 Distribution Characteristics of Velocity Field

3.2.1 Summer Cooling Condition

Under summer cooling conditions, the indoor air velocity shows a vertical stratification characteristic of "high at low levels and low at high levels" (Figure 5). The air velocity in the human core activity zone (0.7m-1.9m) ranges from 0.04m/s to 0.12m/s, with a relatively higher velocity (0.06m/s-0.12m/s) in the near-ground area (0.7m-1.1m), which is consistent with the characteristic of cold air sinking, ensuring effective coverage of the human activity zone by cold air. The air velocity in the upper zone (2.0m-3.0m) decreases significantly to 0.02m/s-0.06m/s, with slow airflow, indicating weak lifting

capacity of cold air and dominant natural convection of hot air in this region.

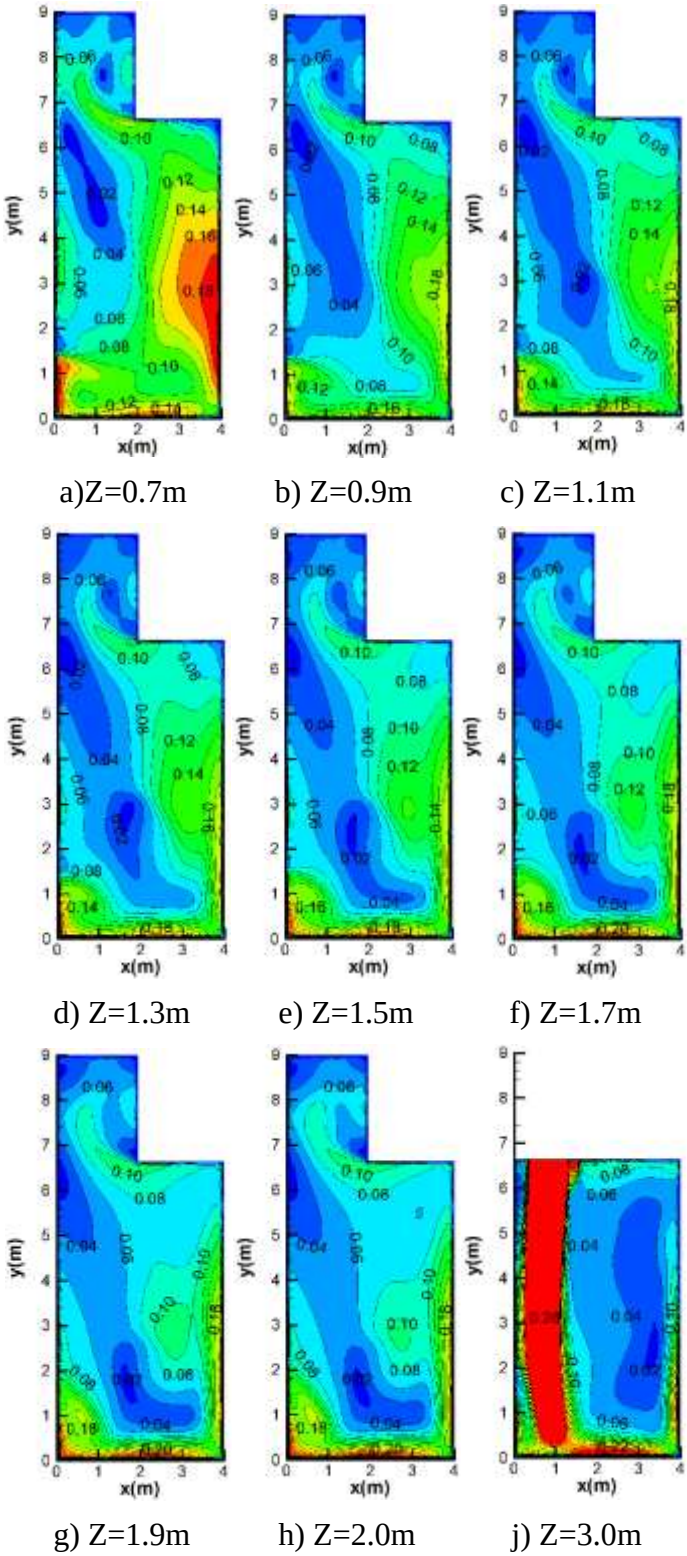

a)Z=0.7m b) Z=0.9m c) Z=1.1m

d) Z=1.3m e) Z=1.5m f) Z=1.7m

g) Z=1.9m h) Z=2.0m j) Z=3.0m

Figure 5 Velocity field distributions at different Z-values under summer cooling conditions (Unit: m/s)

In the horizontal direction, there is an obvious "velocity heterogeneous zone" in the core activity zone: the left area (x≈1-2) has a higher velocity (0.08m/s-0.12m/s), which is the supply air jet zone of the air conditioning outlet; the right area

(x≈3-4) has a lower velocity (0.04m/s-0.08m/s), which is the return flow zone after air diffusion. The overall air velocity meets the requirement of "air velocity ≤0.2m/s in the human activity zone" specified in GB/T 50736-2012. In the upper zone, the velocity distribution is relatively uniform, but extremely low velocity zones (≤0.04m/s) appear in room corners (x≈4, y≈7-8), where stagnant airflow is prone to causing heat accumulation.

3.2.2 Winter Heating Condition

Under winter heating conditions, the indoor air velocity presents a stratification characteristic of "low at low levels and high at high levels" (Figure 6). The air velocity in the human core activity zone (0.7m-1.9m) is generally low (0.02m/s-0.06m/s), with the lowest velocity (≤0.04m/s) in the near-ground area (0.7m-1.1m). The upward movement of hot air makes it difficult for the heating air flow to sink to the near-ground area, resulting in insufficient air movement in the foot region of the human body. The air velocity in the upper zone (2.0m-3.0m) increases significantly to 0.06m/s-0.10m/s, with enhanced air activity, indicating that hot air accumulates in the upper part of the room, forming an airflow stratification of "hot air stagnating at high levels and cold air sinking at low levels".

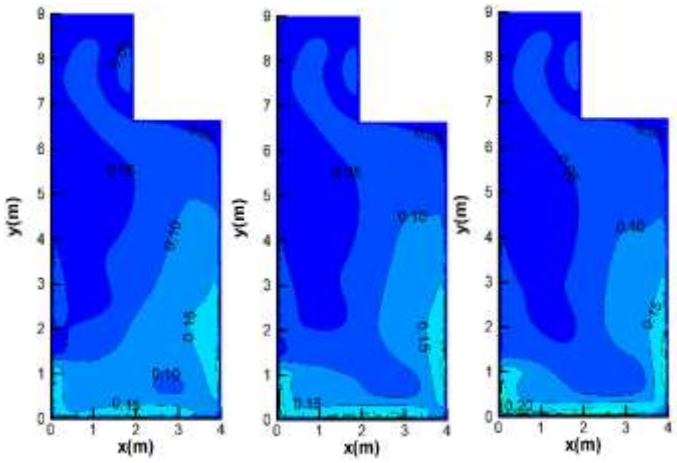

a)Z=0.7m **b) Z=0.9m** **c) Z=1.1m**

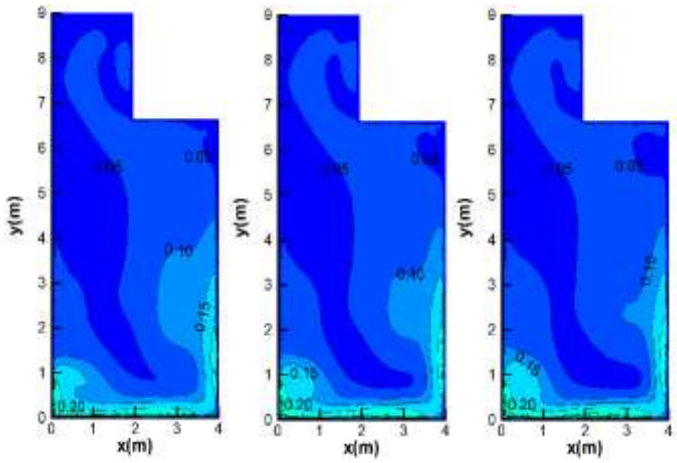

d) Z=1.3m **e) Z=1.5m** **f) Z=1.7m**

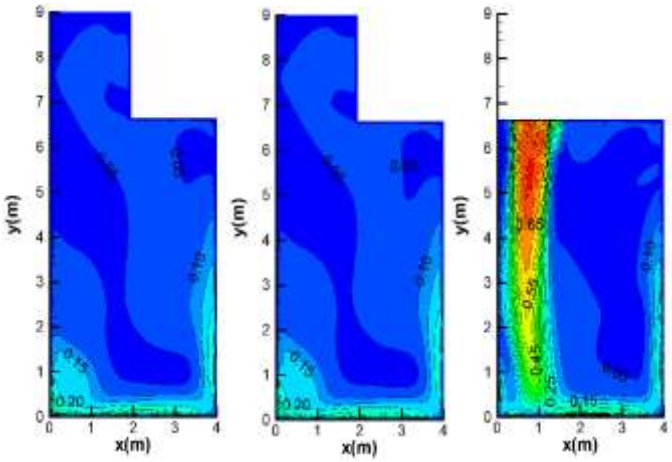

g) Z=1.9m **h) Z=2.0m** **j) Z=3.0m**

Figure 6 Velocity field distributions at different Z-values under winter heating conditions (Unit: m/s)

In the horizontal direction, there is a significant "velocity uneven zone" in the core activity zone: the left area (x≈1-2) maintains a low velocity of 0.02m/s-0.04m/s for a long time, with airflow nearly stagnant, presumably due to being a blind area of the heating air supply or restricted air diffusion caused by wall obstruction; the right area (x≈3-4) has a slightly higher velocity (0.04m/s-0.06m/s). The overall air velocity is below 0.10m/s, without draft sensation, but the low velocity near the ground easily leads to insufficient heat transfer, affecting human thermal comfort. In the upper zone, the velocity distribution is relatively uniform, but a velocity peak (≈0.10m/s) appears in local corners (x≈4, y≈7-8), which is a local convection zone formed during the upward movement of hot air.

3.3 Analysis of the Impact of Solar Radiation

A comparison of the temperature and airflow field characteristics under conditions with and without solar radiation (Figures 7 and 8) shows that in the human activity zone (0-2m), the air velocity in both cases maintains a stable range of 0.06m/s-0.12m/s with small fluctuations, indicating uniform airflow organization. Without solar radiation, the temperature decreases slightly (293.5K-293.2K), while with solar radiation, the temperature remains basically stable at around 293.5K. This indicates that the human activity zone is weakly affected by solar radiation, and the temperature and velocity environments meet the basic requirements of human thermal comfort.

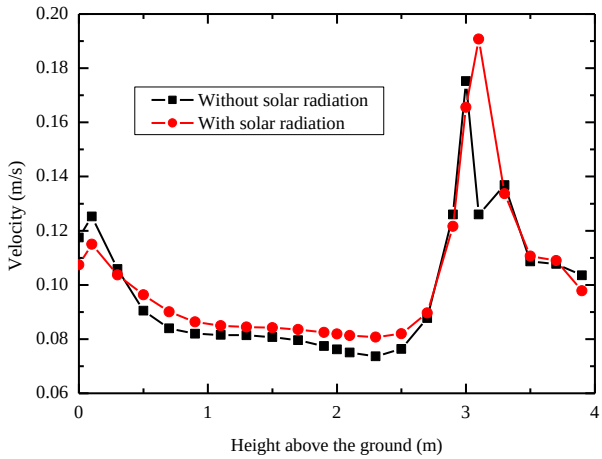

Figure 7 Relationship between air velocity and height above the ground

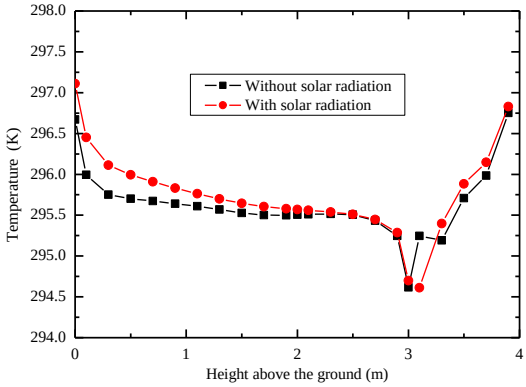

Figure 8 Relationship between air temperature and height above the ground

In the upper zone (2-3m), solar radiation triggers significant fluctuations in "hot air flow-temperature". Without solar radiation, the velocity remains stable (approximately 0.08m/s) and the temperature decreases slowly (293.2K-293.0K), with uniform distribution of temperature and airflow fields. With solar radiation, an obvious temperature "valley" (dropping to 293.0K) appears near 3m, followed by a rapid recovery, accompanied by a synchronous velocity "peak" (approaching 0.20m/s). This phenomenon is the result of the coupling effect driven by thermal buoyancy: on the one hand, solar radiation heats local air, reducing its density and forming upward hot air flow, leading to a sharp increase in velocity in this region; on the other hand, accelerated airflow enhances local heat transfer, temporarily lowering the temperature, and subsequent accumulation of hot air causes the temperature to rise. In summary, solar radiation does not significantly change the temperature and airflow environment in the human activity zone, but has a strong impact on the upper zone above 2m, reducing the air diffusion efficiency of the air conditioning system and increasing energy consumption.

4 Conclusions

In this study, numerical simulation methods were used to systematically investigate the impact of solar radiation on the temperature and airflow fields in a standard double-bed hospital ward in a hot-summer and cold-winter region on the Summer Solstice and Winter Solstice. The main conclusions are as follows:

1. Under summer cooling conditions, the ward temperature presents a distribution characteristic of "stable at low levels, transitional at medium levels, and increasing at high levels", while the air velocity shows "high at low levels and low at high levels". Under winter heating conditions, the temperature exhibits "cold at low levels and hot at high levels", and the air velocity presents "low at low levels and high at high levels". The temperature and velocity parameters in the human core activity zone (0.7m-1.9m) all meet the thermal comfort requirements specified in GB/T 50736-2012.

2. Solar radiation has a negligible impact on the temperature and airflow environment in the human activity zone (0-2m), where the temperature and velocity remain stable. However, it has a significant effect on the upper zone above 2m: thermal buoyancy drives airflow acceleration and severe temperature fluctuations, exacerbating hot air accumulation in summer and strengthening thermal stratification in winter, thereby reducing the air diffusion efficiency and energy utilization efficiency of the air conditioning system.

3. Based on the simulation results, it is recommended that hospital beds in hot-summer and cold-winter regions be preferentially arranged in the middle of the human core activity zone

(x≈2-3m, y≈4-6m), avoiding areas with temperature and velocity heterogeneity such as near external walls, air outlets, and room corners. In the design of air conditioning systems, the layout of air outlets in the upper zone can be optimized or flow guiding devices can be added to mitigate the fluctuations of temperature and airflow fields in the upper zone caused by solar radiation and improve the overall thermal comfort level.

This study reveals the characteristics of temperature and airflow fields in wards under the coupling effect of solar radiation and air conditioning systems, providing a scientific basis for the design optimization of hospital wards in hot-summer and cold-winter regions. However, the influence of actual loads such as hospital beds, personnel, and equipment was not considered. Future research can further explore these factors to improve the conclusions.

References

1. Wen J, et al. Application of vacuum technology in the renovation of hospital drainage lifting systems[J]. Chinese Journal of Vacuum Science and Technology, 2020, 40 (2): 119-123.
2. Li W X, et al. Renovation of hospital building forms under the information age[J]. China Sciencepaper, 2015, 10(13): 1588-1593.
3. Li Y, et al. Current status of acoustic environments in outpatient halls of large general hospitals[J]. Architecture Technology, 2015, 46(9): 810-813.
4. Chen W X,et al. Patient-centered design of medical environments[J]. Chinese Journal of Hospital Administration, 2009,25(3):183-18 6.
5. Zhang S M, et al. Optimization of air distribution in hospital wards in severe cold regions[J]. Journal of Thermal Science and Technology, 2023, 22(5): 489-497.
6. Zhang X L. Research on the design of hospital ward ventilation systems based on air distribution optimization[J]. Technology Innovation and Application, 2025,15(28):10 3-106.
7. Tan B, et al. Numerical simulation, analysis and optimization of air distribution in negative pressure wards based on CFD technology[J]. Science Technology and Engineering, 2022, 22(3): 1117-1121.
8. Ding Y X. Simulation of air distribution in air conditioning systems for long and narrow multi-person wards[J]. Shanxi Architecture, 2024, 50(22): 114-117.
9. Kang Z Q, et al. Numerical Analysis of Ward’s FlowField and Pollutant Distribution and Its Impact ofPatients and Visitors.[J]. Procedia Engineering, 2017, 205, 4122-4128.
10. Jin X N. Research on the effect of air conditioningand ventilation in isolation wards under the epi-demic of COVID-19, Lanzhou Jiaotong University, 2022.
11. Ru Z H. Numerical simulation and optimization ofward air-conditioning based on individual needs,Chongqing University , 2021.
12. Chen H F R. Influence of air supply angle of air condi-tioning in container isolation ward on indoor ther-mal environment and air environment in winter,Donghua University, 2021.
13. Wang L L, et al. Simulation analysis of air distribution in standard double hospital wards[J]. International Journal of Nanoscience, 2024, 23(1):1-9..
14. National Standard of the People's Republic of China. Design code for heating ventilation and air conditioning of civil buildings, GB 50736-2012.